The application of arbitrary incidence laser beams heat treatment temperature field calculation formulas

Kun Ma (马 琨)[1], Junchang Li (李俊昌)[1], Zebin Fan (樊则宾)[1], Jinbin Gui (桂进斌)[1], Yingxiong Qin (秦应雄)[2], and Qiguang Zheng (郑启光)[2]

[1] *University of Science and Technology of Kunming, Kunming 650093*

[2] *State Key Lab of Laser Technology, Huazhong University of Science and Technology, Wuhan 430074*

Received August 12, 2004

Based on the calculation formulas of heat treatment temperature field for an arbitrary incident laser intensity distribution, the transformation intensity distribution of CO_2 laser beam passing an integrating mirror is studied theoretically and experimentally. The derived formulas are applied in laser heat treatment research which is transformed by optical system, and the theoretical calculation results are compared with experimental results. It is shown that the formulas can be used to calculate the laser heat treatment temperature field accurately, and the calculation speed is obviously faster than the numerical calculation methods with the same precision. The calculation software can be used to select proper experiment parameters.

OCIS codes: 140.3390, 140.6810, 000.4430, 140.0140.

In the application of surface characteristics transformation by laser, the practical energy distribution of laser beam arriving at the workpiece surface is very complex. In order to control the laser heat treatment, the laser heat treatment calculation has been an energetic research subject. The heat treatment workpiece is regarded as half-infinite continuous medium with constant physical properties[1−4] is a common used simplifying method. Based on this approximation, a fast temperature field calculation method[4] with arbitrary energy distribution has been deduced, and the laser energy distribution is approximated by the superposition of many rectangle beams. The feasibility of the formula is testified by practical laser heat treatment.

In order to meet the need of different surface characteristics transformation, the laser beam is usually transformed into special shapes. In light beam transformation, various types of integrating transformation mirrors are often used as light transformation optical systems. Because the transformed light has complex interference and diffraction structure, how to correctly illustrate the intensity distributions in different spatial planes behind an optics system for the study of thermal effect is another important subject. Approximating the incidence laser beam by the superposition of TEM_{00} and TEM_{01} ideal laser beams with different intensity proportion, the optical transformation characteristic of an integrating mirror was theoretically discussed in detail[5]. However, the practical laser beam energy distribution is more complex. If the temperature field can be calculated with measured laser beam energy distribution, and the theoretical model is testified by experiments, it will be convenient for the practical applications.

Therefore, based on the arbitrary laser beam heat treatment temperature calculation formulas[4], we deduce the arbitrary laser beam transformation results by integrating reflecting mirror. Furthermore, the output light optical capability from integrating reflecting mirror is testified by kilowatt CO_2 laser system. Using the arbitrary laser beam heat treatment temperature calculation formulas and AC1 phase transformation model[4,6], the carbon steel quenching dimension processed by the transformed laser beam is compared with the theoretical results.

Assume that at time $t = 0$, a laser beam with power density distribution $P(x, y)$ is scanning over the surface of half-infinite body, and the scanning speed of laser beam is $\boldsymbol{V} = v_x(t)\,\mathbf{i} + v_y(t)\,\mathbf{j}$ (where $\mathbf{i}$, $\mathbf{j}$ are respectively x- and y-direction unit vector). If the laser material energy absorption coefficient is ρ_0, approximating the laser beam by the sum of $N \times M$ square sub-beams with the same length of side $(2\Delta d)$ and various powers, each sub-beam is uniform, substituting the error function[7] erf, the temperature field in the half-infinite body can be described as[4]

$$T(x,y,z,t,v) - T_0 = \frac{\rho_0\sqrt{\alpha}}{4k\sqrt{\Pi}} \int_0^t \frac{\mathrm{d}t'}{\sqrt{t-t'}} \exp\left[-\frac{z^2}{4\alpha(t-t')}\right] \times \left\{ \sum_{j=1}^{M} \left[\mathrm{erf}\left(\frac{\Delta d + v_y t' + y_j - y}{\sqrt{4\alpha(t-t')}} \right) - \mathrm{erf}\left(\frac{-\Delta d + v_y t + y_j - y}{\sqrt{4\alpha(t-t')}} \right) \right] \times \sum_{i=1}^{N} p(x_i, y_j) \left[\mathrm{erf}\left(\frac{\Delta d + v_x t' + x_i - x}{\sqrt{4\alpha(t-t')}} \right) - \mathrm{erf}\left(\frac{-\Delta d + v_x t' + x_i - x}{\sqrt{4\alpha(t-t')}} \right) \right] \right\}, \quad (1)$$

where T_0 is the initial temperature of material (K), k is the thermal conductivity ($\mathrm{W \cdot m^{-1} \cdot K^{-1}}$), and α is the thermal diffusion coefficient ($\mathrm{m^2 \cdot s^{-1}}$).

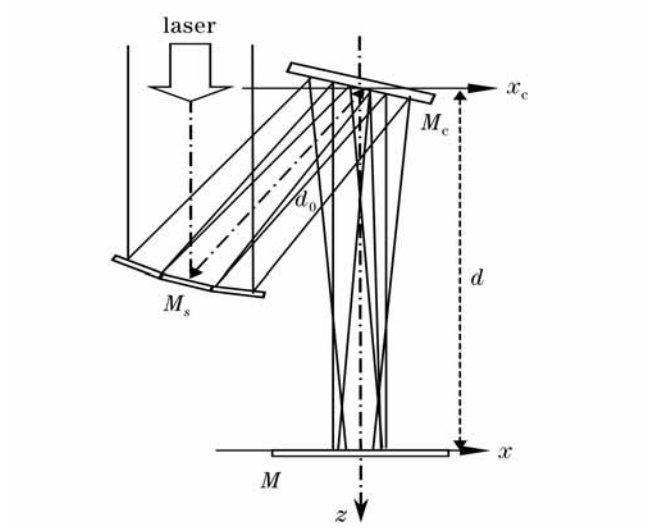

Fig. 1. An integrating reflecting mirror and its coordinates definition.

From Eq. (1), we can see that it is not too difficult to develop a software to resolve it.

Figure 1 shows the transformation principle and coordinates of an integrating reflecting mirror. In the figure, M_s is a cylinder prism mirror composed of three rectangle reflective mirrors which are attached on the surface of a concave mirror. The perpendicular incidence light beam is divided into three beams and reflected to a cylinder mirror M_c by M_s. If the foci of M_s and M_c are respectively f_x and f_y, the focal lines of them are perpendicular with each other. When the light beams are reflected by M_c, narrow strip spot is formed in position near the focal plane. Because the narrow strip spot is formed by the superposition of sub-beams which were divided from the same incidence beam, according to the practical incident intensity, if suitable width of three rectangle planar mirrors are designed, intensity of the narrow strip spot is uniform in x-direction.

In order to testify the above theoretical results, the experiment is fulfilled with a kilowatt CO_2 laser system, the corresponding parameters of laser and integrating transformation mirror are: laser power output 1060 W; integrating transformation mirror parameters $a = 10$ mm, $D = 3a$, $f_x = 238$ mm, $f_y = 160$ mm, $d_0 = 90$ mm. Figure 2(a) is the thermal paper sampling result[8] of incidence laser beam before it reaches the mirror. According to the energy-gray response characteristics, the spatial intensity distribution profile can be obtained by digital image processing, and the result is shown in Fig. 2(c). Figure 2(b) is the heat effect simulation result based on Fig. 2(c). Thus we can simulate the sampling laser beam at any observation position on the thermal paper according to the calculation results, and the theoretical calculation result can be testified directly.

From Fig. 2 we can see that the width of central sub-beams is obviously wider than that of the side ones. Let the laser beam incline $a/2 = 5$ mm to the x-direction, the incidence laser beam is then separated into two beams by the middle mirror and the right mirror. The laser beam spots at two different observation planes with different sampling time Δt are shown in Figs. 3(a) and (d).

From the figure we can see the laser beam intensity

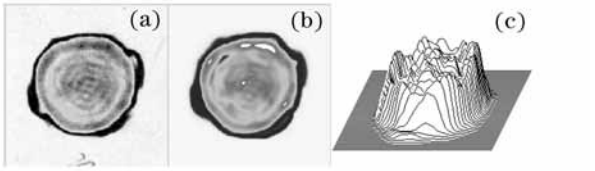

Fig. 2. The sampling (a) and simulation (b) results of laser beam before it reaches the mirror. (c) Spatial intensity distribution profile. 25.6×25.6 mm^2.

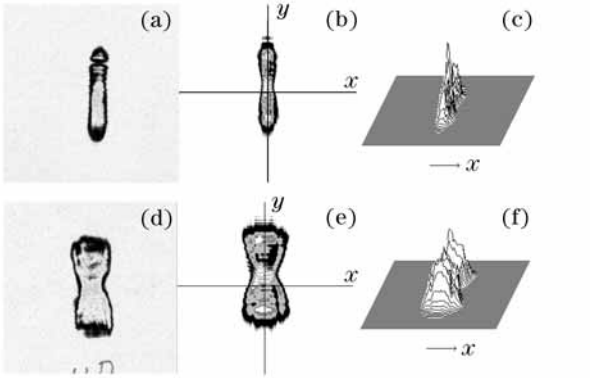

Fig. 3. The sampling (a, d) and simulation results (b, e) of laser beam in different positions, and the corresponding intensity distribution profiles (c, f). 25.6×25.6 mm^2. (a, b, c) $d = 182$ mm, $\Delta t = 30$ ms; (d, e, f) $d = 222$ mm, $\Delta t = 80$ ms.

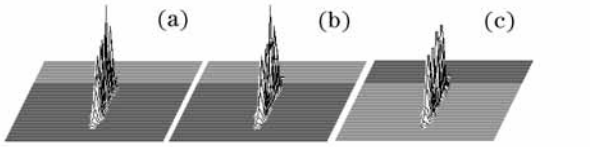

Fig. 4. The spatial distributions of the same laser beam approximated by 256×256 (a), 128×128 (b), and 64×64 (c) rectangle laser beams.

distribution is different in different observation positions. The laser beam has a more narrow strip intensity distribution near the focus plane of the cylinder mirror. The simulation distribution in Figs. 3(b) and (e) are obtained from thermal paper energy-gray response characteristics. The distribution shows good agreement with the experimental results. Figures 3(c) and (f) are the three-dimensional (3D) intensity distribution profiles.

In order to study the laser heat treatment of integrating transformation mirror, based on AC1 phase transformation mode[4,7], laser quenching experiments were carried out on carbon steel (0.45% carbon) surface for three different geometric types with the boundary angle $\theta = 45°$ at $d = 172$ mm on a cuboid workpiece. A 1060-W, 1.06-μm CO_2 laser beam was used. The output spatial intensity distribution from the integrating transformation mirror is shown in Fig. 4, approximated with 256×256 (Fig. 4(a)), 128×128 (Fig. 4(b)), and 64×64 rectangle element laser beams (Fig. 4(c)). We can see that choosing the smaller rectangle element laser beams can approximate, the original laser beam more precisely. Equation (1) can thus be used to calculate the laser beam heat treatment temperature field.

Let laser beam scanning at the speed of 10 mm/s in x-direction, the observation time $t = 2$ s; the phase transformation temperatures AC1 = 760 °C, AC3 = 860 °C,

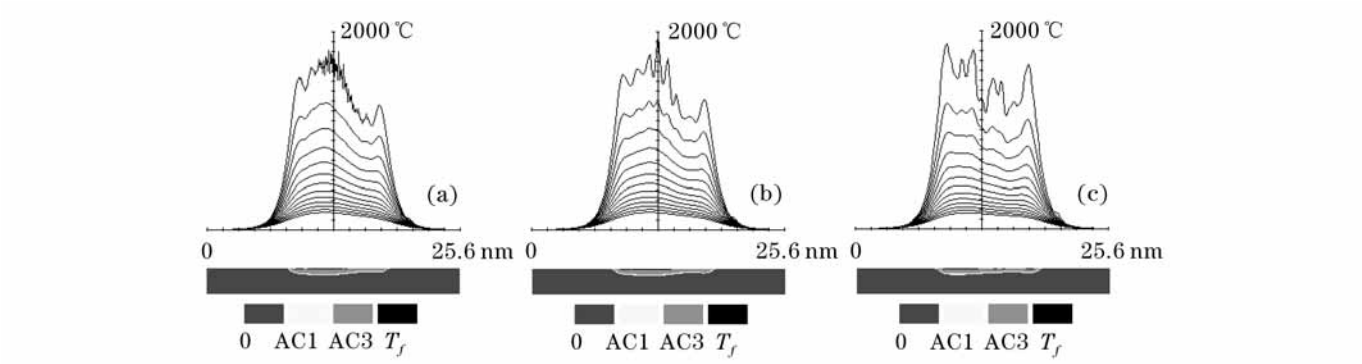

Fig. 5. The calculation time and calculation results of quenching area. (a) 5486 s, 10.3 mm; (b) 1298 s, 10.4 mm; (c) 337 s, 10.8 mm.

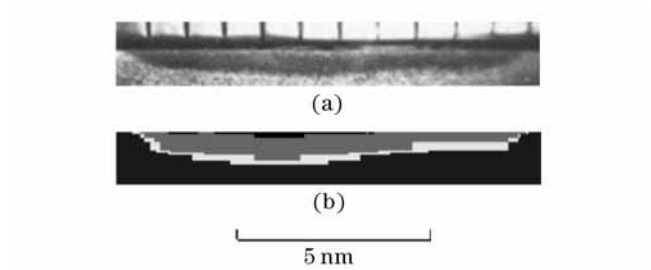

Fig. 6. The theoretical calculation (a) and experimental (b) results of phase hardened area.

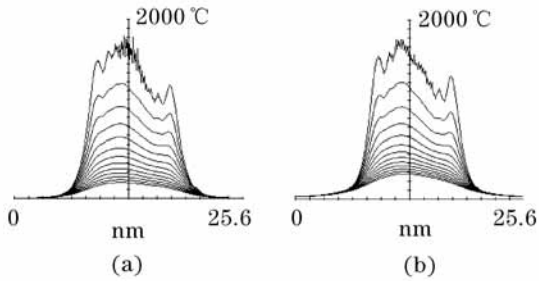

Fig. 7. Comparison between two different calculation methods. (a) By using Eq. (1); (b) by using FFT. Every two adjacent curves are calculated with the spacing of 0.1 mm in the depth direction.

$T_0 = 20$ °C, melting point $T_f = 1500$ °C, $k_0 = 0.026$ W/(mm·K), $\alpha = 4.2$ mm^2/s, and the surface energy absorption coefficient $\rho = 0.7$.

Figures 5(a)−(c) show the calculation time and calculation results of quenching area corresponding to the light spots defined by Figs. 4(a)−(c), respectively.

The calculation results and practical measurement results shown in Fig. 6 manifest that the phase hardened area can be satisfactorily got from the calculation. Besides, the material melt area can be preferably marked out. If a complicated machining workpiece is to be processed, the melt damage of the workpiece can be avoided by the calculation before laser heat treatment. We have done the similar research for many worpieces. Usually the average discrepancy between theoretical calculation and experiment measurement is in the range of 15%. For the present situation, through experiments to optimize heat treatment techniques, this is an encouraging result.

For the calculation of arbitrary laser heat effect calculation, Li *et al.* have presented a high efficient rapid calculation method[4]. The characteristics of this method are summarized at follows. The theoretical research shows that, after the non-limit integral function which has definition in the infinite plane is truncated, sampled, and extended, the rapid-calculation method is to use fast Fourier transform (FFT) to calculate the convolution to fulfill the calculation. When the function truncation is equivalent to import artificial distortion, the limited sampling nodes bring "frequency mixing-superposition"[4]. The "frequency mixing-superposition" leads to the calculation results being approximation of practical value; the calculated temperature is higher than the numerical calculation result in the vicinity of calculation area boundary. Figures 7(a) and (b) show the calculation temperature fields using Eq. (1) and FFT, respectively. The curves express the temperature field distribution at $t = 2$ s, at the section of laser beam back part parallel to the laser beam length direction. From the temperature distribution curves we can see that there is a slight discrepancy in the two calculation methods in the vicinity of calculation area boundary. However, as the temperature distribution curves above AC1 are almost the same, there is no essential difference in the predication of phase hardened area of two methods.

As the above comprison is based on the precondition of the calculation area is regarded as half-infinite body, there is no influence on the calculation of phase hardened area of two methods. Whereas when "image heat source" is used to deal with the boundary condition, if the "frequency mixing-superposition" is not decreased by increasing sampling nodes, the rapid calculation method cannot be used directly. In this case, Eq. (1) is very suitable to calculate the temperature field.

The comparison shows that for non-melting laser heat treatment, the rapid calculation method and semi-analytic calculation method not only present a good agreement with experiment, but also have high efficiency. For example, we have used the same PC with different calculation methods to finish a laser hardening treatment temperature calculation of Fig. 6, the calculation time of finite element method (FEM) is 5 h, the rapid-calculation method needs 54 s; when the laser beam is the combination of 64×64 rectangle laser beams, the calculation time is just 12 min. In fact, just calculating the hardened depth and middle width is sufficient to predict the heat treatment result. Compared with pure

numerical temperature field calculation, the advantage of rapid-calculation method and semi-analytic calculation method are extremely obvious in practical calculation. For a measured incidence laser beam, we adopt 256×256 rectangle laser beams to simulate the laser beam on observation plane, the calculation time of PIII733 is about 10 s, which means that the power density distribution at any observation plane after the optical system can be precisely calculated. When the laser beam is approximately described by the properly chosen amount of rectangle beams, the laser heat action can be calculated in one minute. After the above calculation methods are programmed as combination software with integrating transformation mirror, it is very useful for optimizing the control of laser heat treatment.

This work was supported by the National Natural Science Foundation of China (No. 60178004) and the Natural Science Foundation of Yunnan Province (No. 2000F0042M). K. Ma's e-mail address is makun_box@yahoo.com.

References

1. B. C. Kewarlinke, *The Strength of Hardware by Laser* (in Chinese) D. R. Guo and L. Q. Hu (trans.) (National Defence Industry Press, Beijing, 1985).
2. M. Von Allmen, *Laser-Beam Interactions with Materials Physical Principle and Applications* (in Chinese) H. B. Qi (trans.) (Science in China Press, Beijing, 1994).
3. J. Li, C. Renard, and J. Merlin, Journal de Physique III (in French) **3,** 1497 (1993).
4. J. C. Li, *The Calculation of Laser Diffraction and Thermal Affection* (in Chinese) (Science in China Press, Beijing, 2001).
5. J. C. Li, Q. G. Zheng, D. X. Ling, Y. X. Qin, and C. G. Li, J. Optoelectronics·Laser *13,* 767 (2002).
6. C. Renard, J. Li, T. Manderscheid, and J. Merlin, Revue de Metallurgie (in French) 341 (1991).
7. Y. H. Shen, Z. Z. Liang, L. H. Xu, and Q. Q. Cai, (ed.) *Practical Mathematics Manual* (Science in China Press, Beijing, 1992) p.658.
8. Z. C. Zhu, W. R. Wang, and S. L. Yu, Chin. J. Lasers (in Chinese) **21,** 846 (1994).
9. Q. R. Zhuang, W. Z. Zhang, and F. P. Lü, Chin. J. Lasers (in Chinese) **29,** 271 (2002).